

Polymeric carbon nitride as a metal-free catalyst for NO decomposition

Junjiang Zhu, Yuechang Wei, Wenkai Chen, Zhen Zhao, Arne Thomas

Technical University Berlin, Englische Str. 20, 10587 Berlin Germany

State Key Laboratory of Heavy Oil Processing, Faculty of Chemical Science and Engineering, China
University of Petroleum, Fuxue Road, Chang Ping, Beijing 102249, China

Department of Chemistry, Fuzhou University, Minhou, Fuzhou 350108, China

Supplementary Information

Methods

Synthesis of g-C₃N₄: 4.5 g cyanamide was directly put in a crucible and then calcined at a rate of 2 °C/min from room temperature to 550 °C in air atmosphere. The sample was tempered at 550 °C for another 4 h before cooling down.

Synthesis of g-C₃N₄*: 4.2 g cyanamide was first dissolved in 25 mL de-ionized water with stirring. The pH value of solution measured in this condition is about 4.5. Subsequently, ~0.4 M NaOH was dropped to tune the pH value to ~8.5. After then, the solution was heated at 90 °C until all the water was gone. The resulting sample was dried at 110 °C for several hours and calcined at 550 °C for 4 h (with a heating rate of 2 °C/min).

Synthesis of M-C₃N₄: 4.8g cyanamide was first dissolved in 25 mL de-ionized water with stirring. Subsequently, 1 mL 0.0152 M ZnCl₂ (or HAuCl₄) solution was added. The resulting solution was heated at 90 °C until all the water was evaporated. The resulting sample was dried at 110 °C for several hours and then heated at a rate of 2 °C/min to 550 °C. The sample was tempered at 550 °C for another 4 h before cooling down.

Characterization: The XRD patterns were measured on a Bruker D8 Advance X-ray diffractometer (Cu K α_1 irradiation). Transmission electron microscopy (TEM) was recorded on a FEI Tecnai 20 microscope. UV-vis measurements were measured on a VARIAN 300 SCAN instrument in the range of 200 ~ 800 nm.

Catalytic Reaction: NO removal reactions were carried out on a fixed-bed tubular quartz system. The reaction temperature was controlled through a PID-regulation system based on the measurements of a K-type

thermocouple and varied from 30 to 550 °C. 200 mg sample was placed in the tubular quartz reactor with an internal diameter of 6 mm in each test. Reactant gases containing 4000 ppm NO balanced with He were passed through the catalyst at a flow rate of 50 mL/min. The outlet gas from the reactor passed through a 1 cm³ sampling loop of a six-point gas-sampling valve before it was being injected into an on-line GC, which was equipped with a thermal conductivity detector (TCD) and a molecular sieve 5A column. NO concentration data were collected after the reaction practically reached steady-state at each temperature (ca. 2 hs) and NO conversion was expressed as: $X_{NO} = ([NO]_{in} - [NO]_{out}) / [NO]_{in} * 100 \%$, where $[NO]_{in}$ and $[NO]_{out}$ are the initial and end (at each temperature) NO concentrations, respectively.

Theoretic Calculation: Density functional theory (DFT) was used to simulate the adsorption of NO on C₃N₄. In the computation, the exchange-correlation functional was the generalized gradient approximation of Perdew and Wang (GGA-PW91). The electron wave functions were expanded into a set of numerical atomic orbital by a double-numerical basis with polarization functions (DNP).

The whole calculations were carried out with the Dmol³ code. The adsorption energy E_{ad} is defined as:

$$E_{ad} = E_{NO} + E_{C_3N_4} - E_{system}$$

where $E_{C_3N_4}$ and E_{HCHO} is the total energy of the substrate and adsorbate, respectively, while E_{system} is the total energy of adsorbate-substrate system at the equilibrium state.

Two models were proposed for the adsorption of NO on C₃N₄: one is the parallel adsorption, in which the both two atoms of NO are adsorbing on C₃N₄, as shown in [Figure S10](#); the other one is the erect adsorption, in which only one atom of NO is adsorbing on C₃N₄, as shown in [Figure S13](#).

Table S1: Element analysis (C, H, N) result of the investigated catalysts

Sample	Weight percent (wt. %)			Molecular Formulate
	C	N	H	
g-C ₃ N ₄	33.16	58.0	1.4	C ₃ N _{4.5} H _{1.5}
g-C ₃ N ₄ *	33.1	58.5	1.3	C ₃ N _{4.5} H _{1.3}
Zn-g-C ₃ N ₄	33.8 (32.5) ^a	59.2 (57.0)	1.1 (1.0)	C ₃ N _{4.5} H _{1.2}
Au-g-C ₃ N ₄	35.1	62.1	1.2	C ₃ N _{4.5} H _{1.2}

^a The value in bracket is taken from the used sample.

To prove that side reactions such as $\text{C}_3\text{N}_4 + 6\text{NO} = 3\text{CO}_2 + 5 \text{N}_2$ is not the main reason responsible for NO conversion, the CO/CO₂ concentrations in the reaction were monitored , as shown in [Figure S1](#). Some amounts of CO/CO₂ were detected, but is far smaller than that calculated from the stoichiometric reaction, suggesting that the side reaction indeed is not the main reason responsible for NO conversion, and thus proving that the C₃N₄ matrix acts as catalyst of NO decomposition.

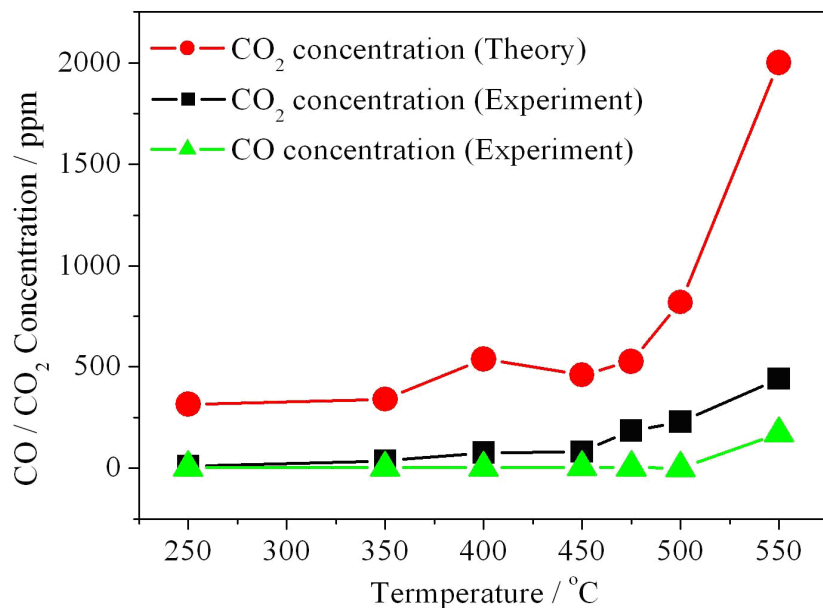


Figure S1: A comparison of CO₂ concentration calculated from stoichiometric reaction ($\text{C}_3\text{N}_4 + 6\text{NO} = 3\text{CO}_2 + 5 \text{N}_2$) and that measured from experiment, together with the CO concentrations detected in the experiment; (Note: CO₂ concentration calculated are based on the above stoichiometric reaction under the flowing reaction conditions: Catalyst: Au-g-C₃N₄; gas: 4000 ppm NO, NO conversion: see [Table 2](#) (at 550 °C the sample show ~100% conversion, which however was not listed in [Table 2](#)))

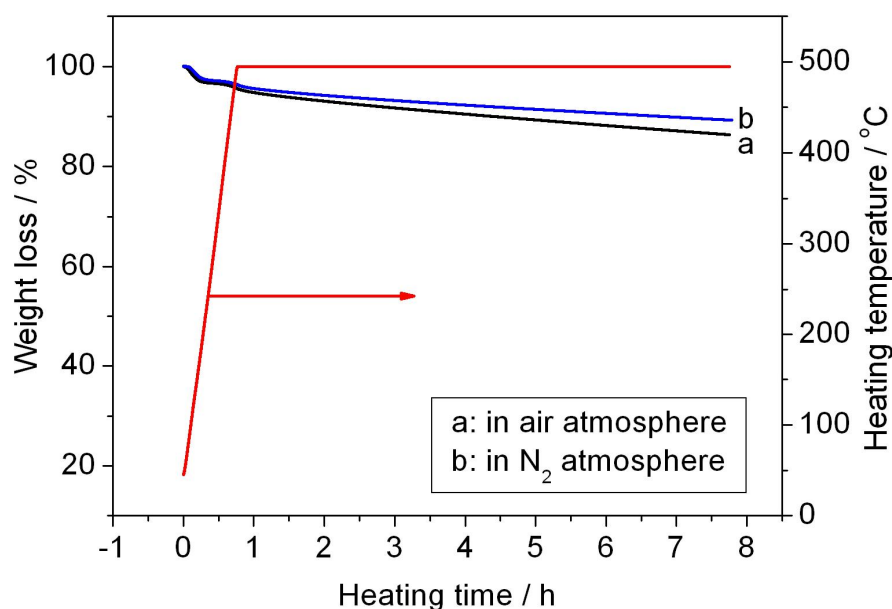


Figure S2: TGA profile of g-C₃N₄ carried out at 500 °C for 8 hs in air and N₂ atmosphere

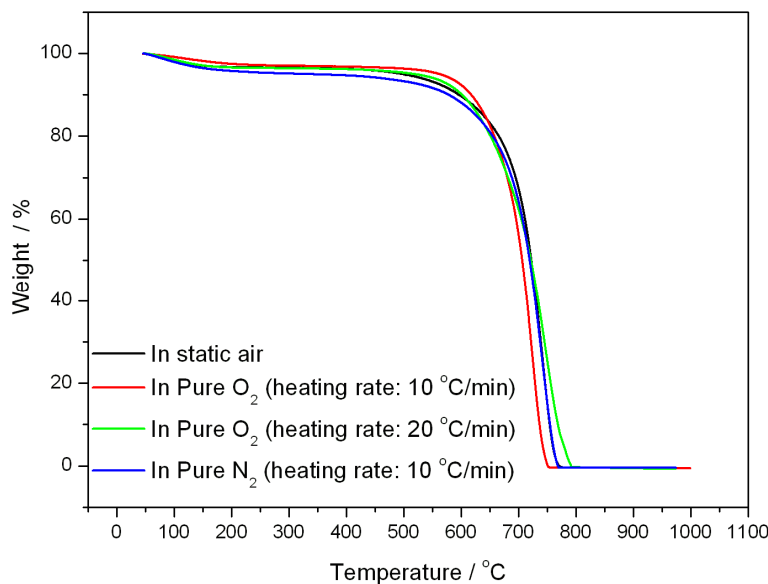


Figure S3: TGA profile of C_3N_4 carried out under different conditions, which shows that C_3N_4 is inert to oxygen even at temperature as high as 550 °C

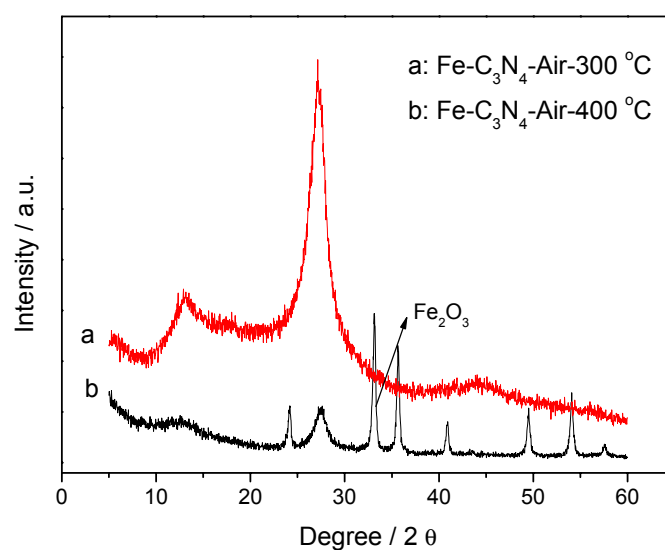


Figure S4: XRD patterns of $\text{Fe-C}_3\text{N}_4$ calcined at 300 °C and 400 °C, which shows that the C_3N_4 matrix structure was largely destroyed after 400 °C.

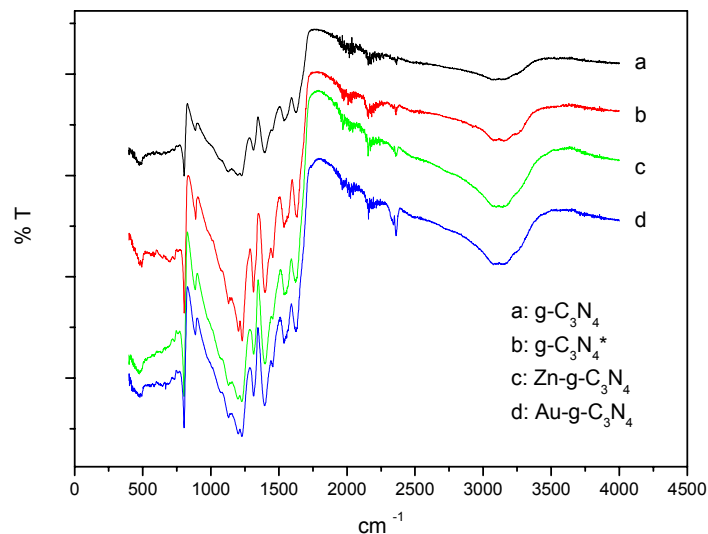


Figure S5: FTIR spectra of the investigated samples. No difference in the samples before and after the incorporation of metal ions was observed, except the peak intensity, suggesting that the matrix structure of all the samples is $\text{g-C}_3\text{N}_4$.

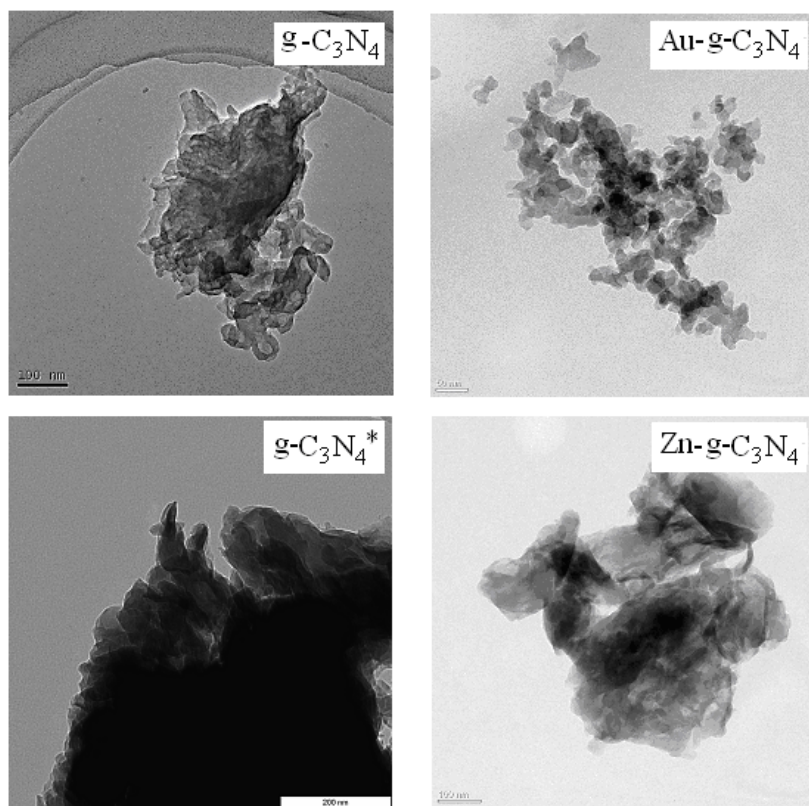


Figure S6: TEM images of the investigated samples, which shown that all the samples featuring a stacking status.

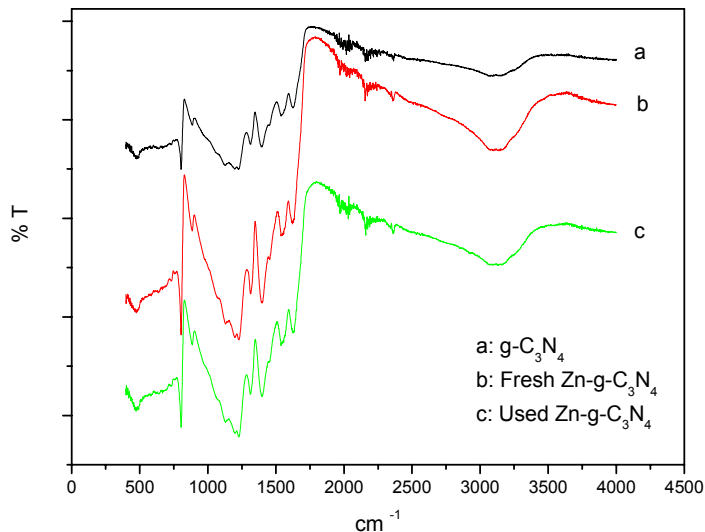


Figure S7: FTIR spectra of $\text{g-C}_3\text{N}_4$, fresh $\text{Zn-C}_3\text{N}_4$ and used $\text{Zn-C}_3\text{N}_4$. No appreciable difference was observed in $\text{Zn-g-C}_3\text{N}_4$ before and after the reaction, suggesting that the oxidation state of Zn is not changed, and hence Zn is not an active site of catalytic redox reaction.

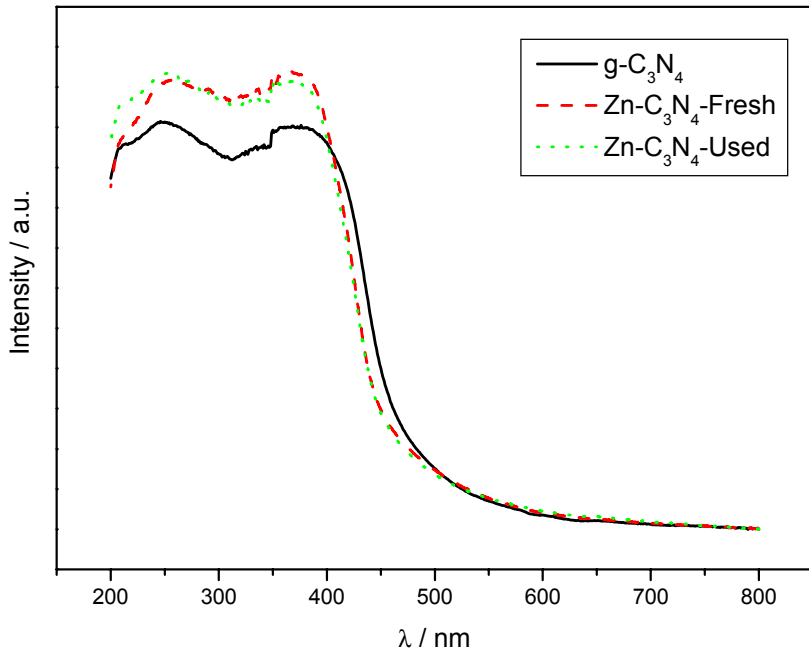


Figure S8: UV-vis spectra of $\text{g-C}_3\text{N}_4$, fresh $\text{Zn-C}_3\text{N}_4$ and used $\text{Zn-C}_3\text{N}_4$. The increase in intensity between C_3N_4 and $\text{Zn-C}_3\text{N}_4$ indicates the incorporation of Zn in the C_3N_4 matrix structure, which is in accordance with that reported previously,¹ while the similar absorption curves of $\text{Zn-C}_3\text{N}_4$ before and after reaction suggests that the electron transition of Zn^{2+} does not happen. That is, the reduction of Zn^{2+} to Zn^0 did not happen after the reaction.

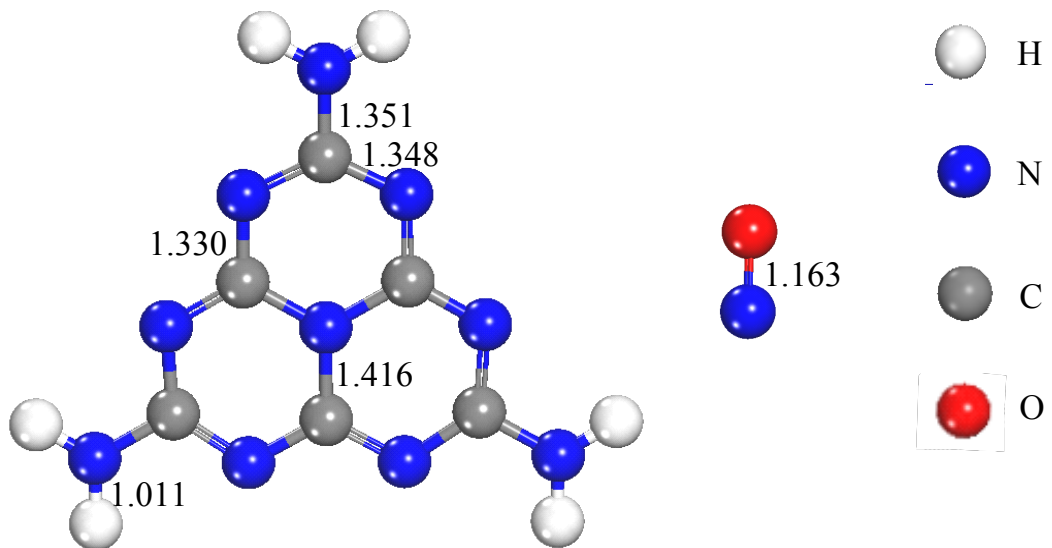


Figure S9: Structural parameters of free NO and C_3N_4 molecule

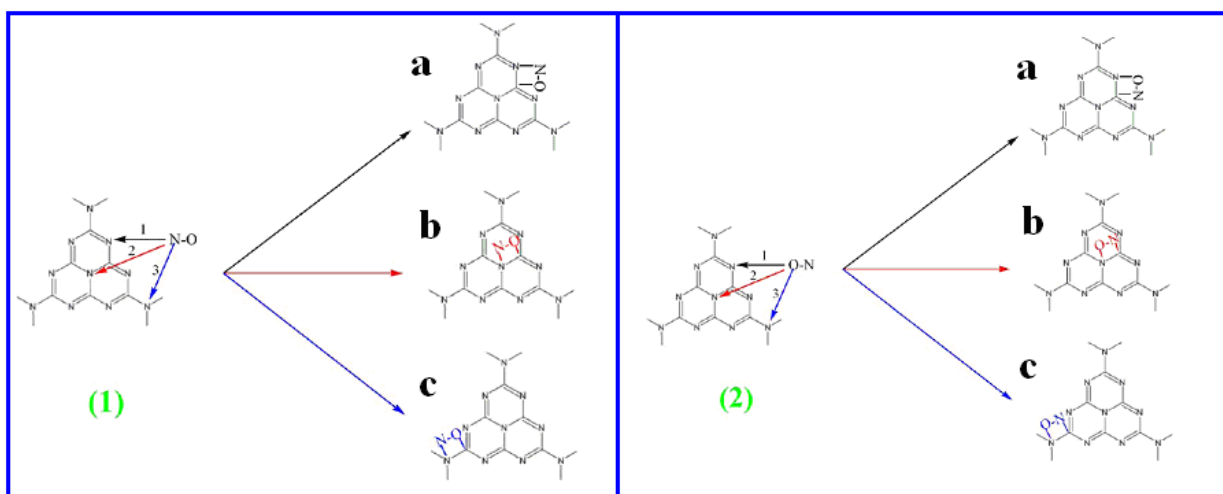


Figure S10: A parallel adsorption model of NO on C_3N_4 . (1) The N atom of NO is adsorbed on the N site, while that of O atom is on the C site of C_3N_4 ; (2) The N atom of NO is adsorbed on the C site, while that of O atom is on the N site of C_3N_4

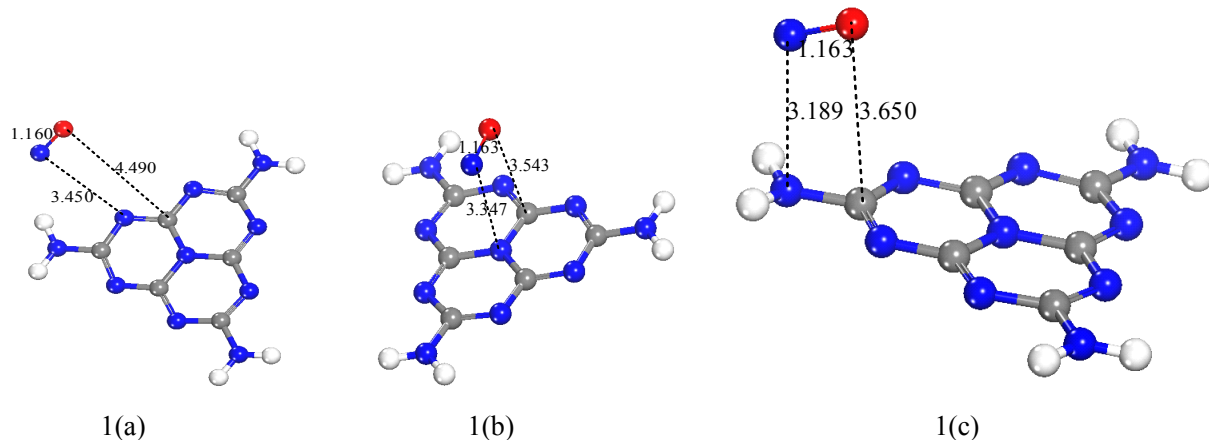


Figure S11: Calculated results from model (1), which indicate that the length of N-O bond is almost unchanged before and after being adsorbed on C_3N_4

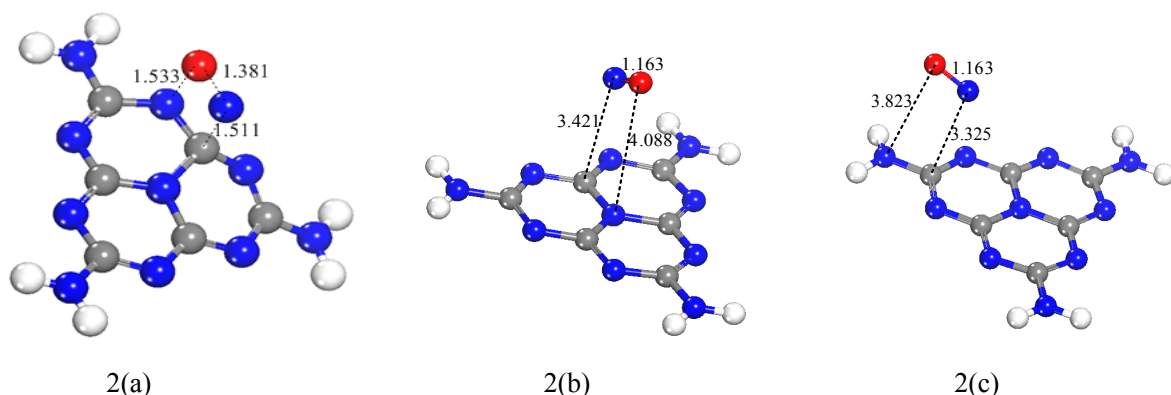


Figure S12: Calculated results from model (2), which show that the length of N-O bond in model (2) *a* is elongated to 1.381 Å after adsorption, suggesting the rupture of N-O bond; while that in model *b* and *c* is almost unchanged before and after being adsorbed on C_3N_4

Table S2 : Calculated results from model 1 and 2

Energy	Model					
	(1) a	(1) b	(1) c	(2) a	(2) b	(2) c
$E_{\text{total}}/\text{Ha}$	-909.840869	-909.838971	-909.839440	-909.707708	-909.831838	-909.839326
E_{sys}/Ha		$E_{\text{NO}}=-129.915124$			$E_{\text{sub}}=-779.921514$	
$E_{\text{ads}}/\text{kJ.mol}^{-1}$	11.11	6.13	11.11	-338.51	-11.11	6.13

$$E' = E_{\text{NO}} + E_{\text{sub}} = -909.836638 \text{ a.u.}$$

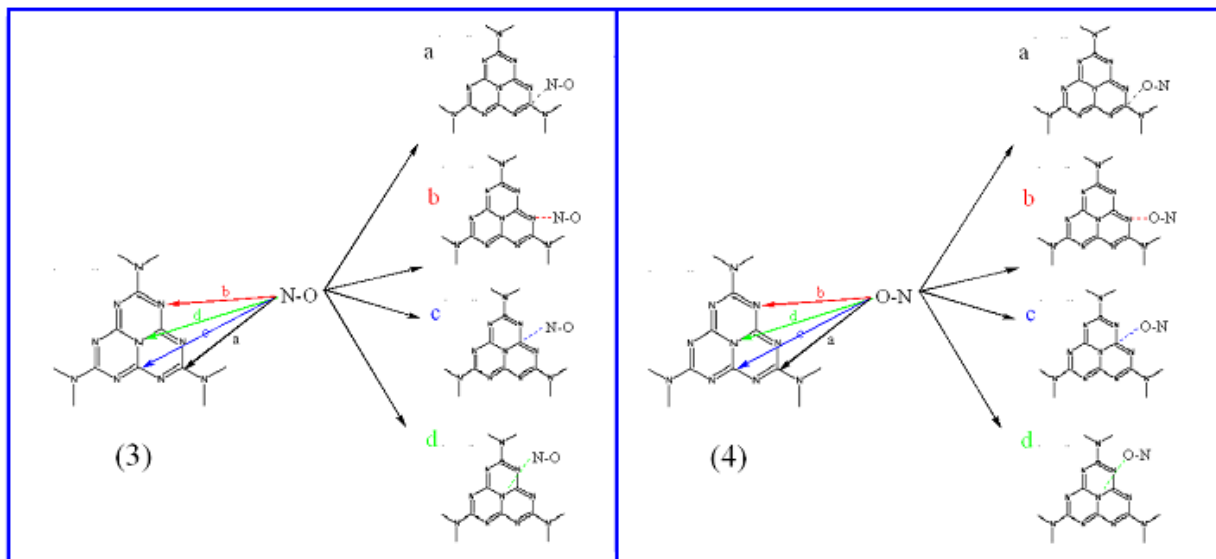


Figure S13: An erect adsorption model of NO on C_3N_4 . (3) The N atom of NO is adsorbed on the N- or C-site of C_3N_4 ; (4) The O atom of NO is adsorbed on the O- or N-site of C_3N_4

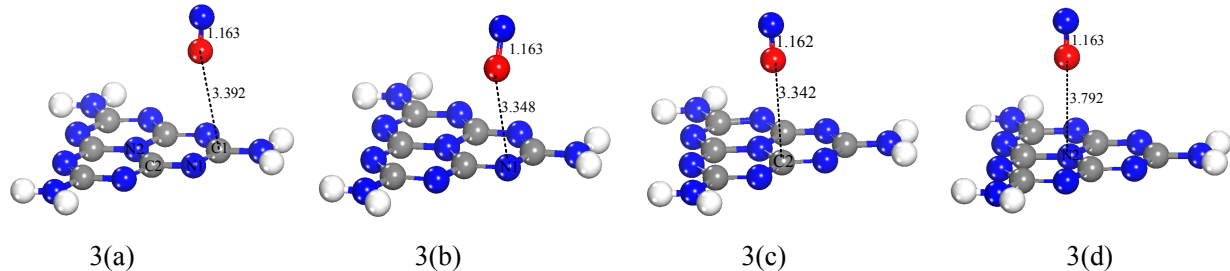


Figure S14: Calculated results from model (3), which indicate that the length of N-O bond is almost unchanged before and after being adsorbed on C_3N_4

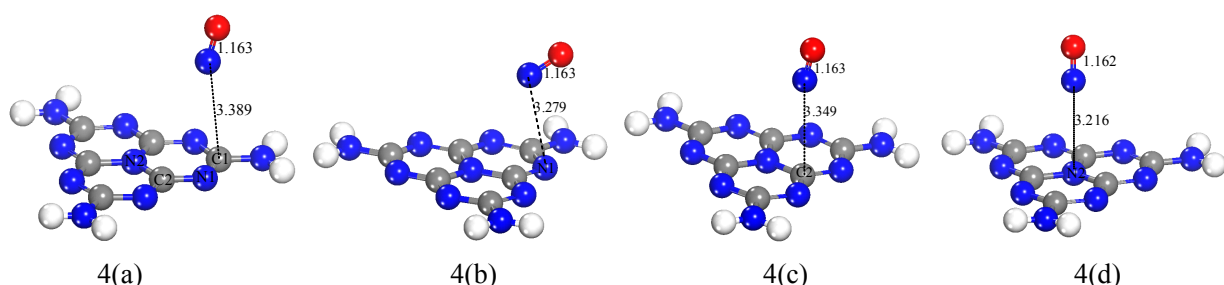


Figure S15: Calculated results from model (4), which indicate that the length of N-O bond is almost

unchanged before and after being adsorbed on C₃N₄

Table S3: Calculated results from model 3 and 4

Energy	Model							
	(3) a	(3) b	(3) c	(3) d	(4) a	(4) b	(4) c	(4) d
E _{total} /Ha	-909.838803	-909.838546	-909.838941	-909.838745	-909.839027	-909.839479	-909.839267	-909.839081
E _{sys} /Ha			E _{NO} =-129.915124			E _{sub} =-779.921514		
E _{ads} /kJ.mol ⁻¹	6.30	7.61	7.09	6.56	5.51	4.99	6.04	5.51

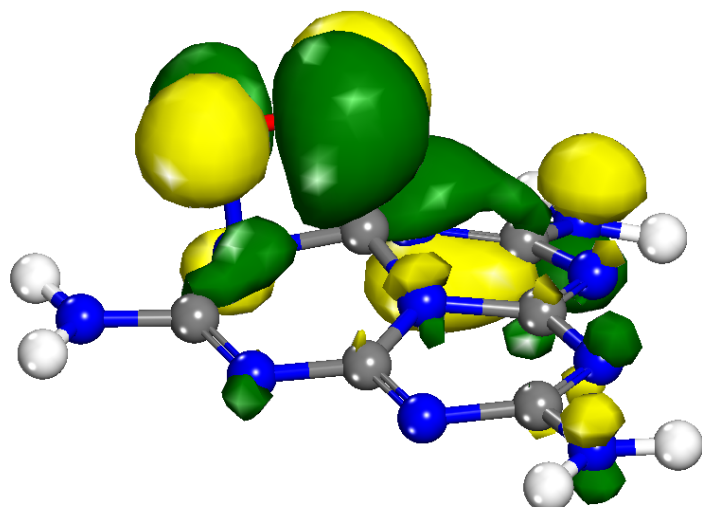


Figure S16: Theoretic simulation on the Mulliken charge distribution of NO before and after adsorption on g-C₃N₄

References

- (1) Wang, X. C.; Chen, X. F.; Thomas, A.; Fu, X. Z.; Antonietti, M. *Advanced Materials* **2009**, *21*, 1609.